Reversible Reactions over Non-metallic Catalysts: A Transient Isotopic Tracing of the Isobutane–Isobutene–Hydrogen System over Chromia

JUO-YU KAO,* HÉLÈNE PIET-LAHANIER,† ERIC WALTER,† AND JOHN HAPPEL‡,1

*American Cyanamide Company, 1800 Valley Road, Wayne, New Jersey 07470; †Laboratoire des Signaux et Systèmes, CNRS-ESE, Plateau de Moulon, 91192 Gif-sur-Yvette Cedex, France; and ‡Department of Chemical Engineering, Columbia University, New York, New York 10027

Whether a single rate-controlling step exists in complex reversible heterogeneous catalytic reactions is difficult to establish, especially with non-metallic catalysts, which often possess fewer active sites than supported metals. This problem is treated here using transient isotopic tracing with ^{13}C marking for the system isobutane–isobutene–hydrogen over a chromia catalyst. A statistical approach is employed for modeling the simultaneous occurrence of traced isobutane and isobutene in the product stream using the Horiuti–Polanyi, mechanism. We find that a single rate-controlling step that consists of the conversion of the half-hydrogenated chemisorbed species $i\text{-}C_4H_9l$ to chemisorbed isobutene $i\text{-}C_4H_8l$ and the reverse exists. Such information should be useful for catalyst design and prediction of performance. © 1992 Academic Press, Inc.

INTRODUCTION

Basically two types of heterogeneous catalytic reactions have been widely studied for both fundamental understanding and practical applications. First there are those that are characterized by a set of unidirectional steps. These include such reactions as the cracking of petroleum compounds and their oxidation. The second class of systems are those in which reversible reactions such as the synthesis of ammonia and of sulfuric acid as well as dehydrogenation and isomerization reactions occur. Tracer studies have been almost entirely devoted to unidirectional reactions, and particularly those involved in the hydrogenation of carbon monoxide according to the well-known Fischer–Tropsch synthesis. Nearly all these studies have involved the use of metallic catalysts, in which the surface concentrations of adsorbed intermediates are relatively high. Here we treat the ^{13}C tracing of reactions among mixtures of isobutane, isobutene and hydrogen using a chromia catalyst as representative of non-metallic species. The reactions studied are reversible. Hence they proceed at a slower rate as equilibrium is approached. These two features necessitate special modifications in both experimental and theoretical treatment.

Tracer studies of heterogeneous catalytic systems can serve two purposes. Some are directed to the establishment of mechanisms involved and may be applied to the development of improved catalysts based on knowledge of factors controlling slow steps. Another use of tracer studies lies in the construction of kinetic rate equations with more than an empirical basis.

Transient isotopic tracing affords special advantages compared to steady-state tracing for access to the fundamental parameters in a heterogeneous catalytic system (1). In such studies, a traced species is substituted for one that is untraced (or the reverse) while at the same time the overall catalytic reaction itself remains unchanged, provided

1 To whom correspondence should be addressed.

that isotopic kinetic effects can be ne-
glected. It is assumed that the rates of che-
misorption or desorption from the gas phase
are much slower than the redistribution of
adsorbed surface species. By study of a
steady-state reaction under given ambient
conditions, one is able to assess the magni-
tudes of individual step velocities and con-
centrations of adsorbed surface species re-
gardless of the overall kinetics, which is
usually written in terms of the effect of
changes in pressure, temperature, and con-
centrations of terminal species (reactants
and products).

In studies involving conventional kinet-
ics, it is often assumed (LHHW models)
that a single rate-controlling step exists for a
given mechanism. It is very difficult to test
the validity of this assumption because often
a number of possible mechanisms may be
considered, each comprising a number of
elementary mechanistic steps. By using
transient tracing (1) it is possible to provide
a sharper identification of whether a single
rate-controlling step exists in such a com-
plex reversible heterogeneous reaction.
This was one of the main purposes of the
present study.

Preliminary findings were presented at the
9th International Congress on Catalysis (2).
In the present paper we include results ob-
tained using important additional refine-
ments in experimental procedure and data
interpretation, as described in what follows.

METHODS

Experimental Procedure

A gradientless recirculating open-flow re-
actor (Fig. 1) similar to those that we had
employed previously (1) was used. The ad-
vantage of a recirculating reactor is that it
can approximate a well-mixed system, so
that a fixed reaction rate can be obtained at
steady state, similar to that obtainable in
a continuous stirred tank reactor (CSTR).
Using a diaphragm pump (Metal Bellows
Corp. MB-41), gas was recirculated at a rate
of 6000 ml/min. The internal recirculation
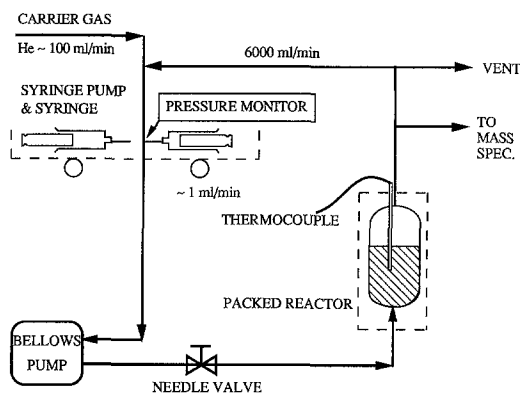rate was approximately 60/1, corresponding

FIG. 1. Schematic diagram of recirculating reactor.

to a forward flow of 100 ml min^{-1}. Dead
space in the reactor system was usually be-
tween 100 and 160 ml depending on size of
the reactor, amount of catalyst, and charge
of inert glass beads. Mean residence times
in the total dead space of the system were
60 to 90 s under our experimental condi-
tions. For satisfactory resolution, it is desir-
able that concentrations of intermediates be
as high as possible relative to amounts of
unadsorbed species circulating in the reac-
tion system. In the case of non-metallic cata-
lysts, concentrations of intermediates are
smaller than for supported metals, so rela-
tively larger quantities of catalyst were re-
quired in this investigation (up to 20 g).

The catalyst employed here was unsup-
ported chromia gel prepared by the proce-
dure described by Emmett and Cines (3), in
which the gel is precipitated from a solution
of chromic nitrate using excess ammonium
hydroxide. The gel was dried slowly for 3
days at 423 K. Surface area by the Bru-
nauer–Emmet–Teller (BET) method was
261 m^2 g^{-1}. Before each experiment, the
catalyst was reduced with hydrogen at 633
K for 12 h and then purged with helium at
the same temperature for 6 h. Amorphous
chromia gel rather than chromia alumina
was used because it possesses a substan-
tially higher concentration of active surface
sites (roughly four times).

The void fraction of the catalyst particle

was estimated to be 0.57 ± 0.08 using the procedure described by Kao (4), with n-hexane as a wetting liquid. The particles were sized to an average diameter of about 2 mm. External diffusion resistance was negligible because of the high recirculation rate (particle N_{Re} = 50,000). Intraparticle resistance was checked by computation of the modified Thiele modulus and found to be typically equal to 0.005. Application of this modulus specifies that the effectiveness factor for a catalytic reaction will be greater than 0.95, if this modulus is less than unity.

Two syringe pumps (100 ml, Sage Instruments Model 351) were installed in tandem on a sliding stand such that the switch from the non-tagged inlet to the labeled stream was completed almost instantaneously. This switching technique minimized pulsation to the entering stream because no valve was employed. Pressure at the reactant injection point could be monitored by inserting a needle probe into the flowing stream. This pressure reading was maintained at atmospheric with a deviation of less than ±1 ml of mercury by adjusting the opening of a Teflon needle valve installed at the outlet of the bellows pump. The needle diameter of the syringe pumps was found to be critical. Tubular flow rate is proportional to the fourth power of the diameter and also depends on the nature of the gas stream being fed. If the diameter is too small, the pressure at the upstream side will cause leakage around the piston seal. However, if it is too large the pressure drop between the reservoir in the piston and the flowing stream in the apparatus will be so small that the rate of delivery will fluctuate due to the inability to control the pressure inside the vessel with sufficient precision. In our studies, a 1-in. (2.54 cm)-length Yale Gage 25 (i.d. ≈ 0.18 mm) was employed.

Another item that was given considerable attention was the employment of additional insulation and an electric heating coil. Details are given by Kao (4). Temperature was monitored by inserting several thermocouples into the top, center, and bottom of the catalyst bed as well as between the insulating layer and the heating coil. With these refinements, it was possible to reduce the longitudinal gradient to 2.4 K over an 8-cm depth of packed column and the radial gradient to less than 1 K across the 1.7-cm radius. Therefore an isothermal recirculating reactor was reasonably approximated. Steady-state tracing levels of reactor effluent were independently confirmed by thermodynamic calculations.

Gas analyses were conducted in a manner similar to that previously described (5). A Finnigan quadrupole mass spectrometer (type 1015C) was employed to analyze the gas composition on line. The electron energy used was 25 eV, and the ionization current was 100 μA. Fragmentation patterns of the pure species, as well as mixture samples, were analyzed separately. It was found that for a mixture of isobutane–isobutene–hydrogen the intensity versus concentration relationships sometimes deviated from linearity, due possibly to interactions among molecular fragments. Calibration was made by independent gas chromatographic analysis, using a Perkin–Elmer Model 900 with helium carrier gas and a flame-ionization detector.

Dead space (CSTR gas phase holdup) was determined by both static and dynamic measurements. In static tests, a gas sample of known volume was injected into the system and the pressure was measured. In dynamic measurements, argon step-up and step-down tests were conducted. These experiments were conducted at a bed temperature close to those of tracer experiments.

Data Interpretation

As discussed in the result section, we first considered a series of model structures, each new structure a simplification of the previous one. In order to select the simplest appropriate model structure, it was necessary to estimate the parameters for each of them. For that purpose, the data were interpreted using the unweighted non-linear least squares criterion, which is the most com-

monly used method for correlating data, so that we thought it should be used as a reference method. As discussed under Results, this procedure showed that the best models for all structures gave almost exactly the same predictions, so that the simplest model structure was selected for making more elaborate statistical calculations. These calculations address the problem that arises when using the least-squares criterion in a situation like this where more than one set of responses is obtained in each experiment, because it is not known what relative weight should be given to the separate sets of data. One way of circumventing this difficulty is to use Box and Draper's determinant criterion (6–8), which is as straightforward as unweighted least-squares. We used the determinant criterion as a second method to estimate the parameters of the structure selected.

A further problem after estimating the values of the parameters is to assess the uncertainties of these values. A conventional way of doing this, which we followed for the least-squares estimates, is to use the Fisher information matrix to compute estimated standard deviations for each parameter. The determinant approach also produces a model of the noise corrupting the data. This gives us the possibility of assessing the uncertainty of the parameters by a Monte Carlo approach (see, e.g., (9)).

The tracer output appears in both isobutane and isobutene. It is therefore convenient to express it as a two-dimensional vector $y(t)$. Let $y_m(t, \theta)$ be the corresponding model output, where θ is the vector of the parameters to be estimated. In the determinant criterion approach, the estimate $\hat{\theta}_{det}$ is obtained by minimizing the criterion

$$j(\theta) = \det D(\theta) \qquad (1)$$

with respect to θ, where $D(\theta)$ is a 2 × 2 matrix given by

$$D(\theta) = \frac{1}{N} \sum_{i=1}^{N} [y(t_i) - y_m(t_i, \theta)][y(t_i) - y_m(t_i, \theta)]^T, \qquad (2)$$

with N the number of measurement times t_i. $D(\theta)$ corresponds to the sample covariance of the error between the measurements and corresponding model output. When there is only a single measurement at time t_i ($i = 1, \ldots, N$), y becomes a scalar and the determinant criterion reduces to the unweighted least-squares criterion. This refinement is therefore of interest here because we observe the markings of more than a single species, in this case isobutane and isobutene.

$\hat{\theta}_{det}$ is the maximum-likelihood estimate of θ under the hypothesis that the data satisfy

$$y(t_i) = y_m(t_i, \theta) + n(t_i),$$
$$(i = 1, \ldots, N), \qquad (3)$$

where the $n(t_i)$ ($i = 1, \ldots, N$) are independently identically distributed Gaussian vectors with zero mean and (unknown) covariance Σ. The maximum-likelihood estimate of this covariance is then simply given by

$$\hat{\Sigma}_{ml} = D(\hat{\theta}_{det}). \qquad (4)$$

The unweighted least-squares estimate of θ is a maximum-likelihood estimate if $\Sigma = \sigma^2 I$, where I is the identity matrix, which is a more restrictive hypothesis than that used in the determinant approach. The determinant criterion therefore has the advantage of being more general while keeping the same number of parameters in the optimization problem. A further advantage of this approach is that the parameters of the deterministic part of the model (θ) and of the noise (Σ) are estimated by minimizing a criterion that is a function of θ only.

If one could repeat the same experiment several times, one would obtain different data sets because of the random perturbations involved. By estimating the parameters associated with each of these data sets, one could obtain an idea of the variability in the estimates due to the variability in the data. The basic idea of Monte Carlo analysis is to replace actual experiments by simulations of the best available model. This approach has the advantage over the use of the Fisher information matrix of not relying on asymptotic results on the convergence prop-

erty of maximum likelihood estimators (at the cost of requiring much more computation). For each run, 500 simulated data sets were generated by computing

$$\mathbf{y}_s(t_i) = \mathbf{y}_m(t_i, \hat{\boldsymbol{\theta}}_{det}) + \mathbf{n}_s(t_i, \hat{\Sigma}_{ml}),$$
$$(i = 1, \ldots, N), \quad (5)$$

where the simulated "measurement errors" $\mathbf{n}_s(t_i, \hat{\Sigma}_{ml})$ $(i = 1, \ldots, N)$ were pseudo-randomly generated according to a Gaussian distribution with zero mean and covariance $\hat{\Sigma}_{ml}$. Five hundred pseudo-estimates θ^k were then computed by minimizing the determinant criterion for each of these simulated data sets. Finally, the mean $\langle \theta_i \rangle$ and standard deviation σ_i of the ith component of the parameter vector over the population of pseudo-estimates thus obtained were computed according to

$$\langle \theta_i \rangle = \frac{1}{500} \sum_{k=1}^{500} \theta_i^k \quad (6)$$

and

$$\sigma_i = \left[\frac{1}{499} \sum_{k=1}^{500} (\theta_i^k - \langle \theta_i \rangle)^2 \right]^{1/2}. \quad (7)$$
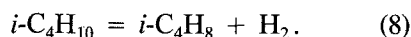
RESULTS

In studying this reversible reaction by transient tracing, there are eight basic types of experiments that can be conducted. For the isobutane–isobutene–hydrogen system, one can study either hydrogenation or dehydrogenation. Second, it is possible to label either isobutane or isobutene with ^{13}C, provided that both are present in the feed. Finally it is possible to conduct an experiment using either step-up, in which the marked species is substituted abruptly in place of unmarked species at the beginning of a transient test, or a step-down, where the reverse procedure is used after operation at steady state with tracer.
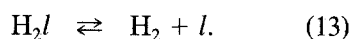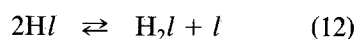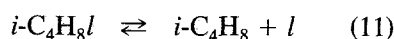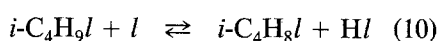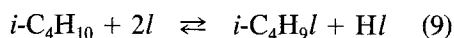
In the course of these studies, all these modes of operation were employed to ensure that consistent results were being obtained. Greater precision was achieved by reactant labeling because the amount of

traced species was higher, so this procedure was adopted in recent experiments aimed at the most accurate determination of parameters. In a step-up experiment the initial conditions correspond to natural abundance of the ^{13}C. In a step-down experiment, however, initial conditions are obtained from measurements at the final marking level of a previous step-up experiment that has been operated for a time sufficient to approach steady state. Thus error in the initial condition for a step-down experiment can be inherited from its previous step-up. Therefore the step-down procedure was infrequently employed. With these factors considered, we selected six typical data sets as representative of our most recent data. The transient tracing conditions of these data sets are summarized in Table 1.

In our study we assumed the well-known Horiuti–Polanyi (10) mechanism involving the half-hydrogenated state. The overall reaction is

$$i\text{-}C_4H_{10} = i\text{-}C_4H_8 + H_2. \quad (8)$$

It consists of the following elementary steps:

$$i\text{-}C_4H_{10} + 2l \rightleftarrows i\text{-}C_4H_9l + Hl \quad (9)$$

$$i\text{-}C_4H_9l + l \rightleftarrows i\text{-}C_4H_8l + Hl \quad (10)$$

$$i\text{-}C_4H_8l \rightleftarrows i\text{-}C_4H_8 + l \quad (11)$$

$$2Hl \rightleftarrows H_2l + l \quad (12)$$

$$H_2l \rightleftarrows H_2 + l. \quad (13)$$

Here l denotes a site for chemisorption. For this reaction both hydrogenation and dehydrogenation may be conveniently conducted at a temperature near 623 K over chromia gel catalyst. The molecular species involved when ^{13}C is used as a tracer are i-C_4H_{10}, i-C_4H_9l, i-C_4H_8l, and i-C_4H_8. Each of these molecular species constitutes one pool in a transient-tracing compartmental model (Fig. 2a). The ordinary differential equations associated with this *four-pool model* are obtained by material balances for tracer species over each of the compartments (1):

TABLE 1

Transient Tracing Conditions

Run No.:	0725A88	0717A88	1030A87	0725B88	0717B88	1031A87
Tracer	Butane	Butane	Butane	Butene	Butene	Butene
Reaction	Dehyd.	Dehyd.	Dehyd.	Hyd.	Hyd.	Hyd.
Temperature (K)	627	629	630	628	630	628
V(ml g^{-1} min^{-1})	0.01602	0.00529	0.00402	−0.00734	−0.01443	−0.009118
W (g)	16.63	16.63	20.07	16.63	16.63	20.07
β (ml)	141	141	183	141	141	183
P (mm Hg)	781	781	771	781	781	776
i-C$_4$H$_{10}$ inlet (ml min^{-1})	1.000	0.762	0.740	0.200	0.000	0.000
i-C$_4$H$_{10}$ outlet (ml min^{-1})	0.734	0.674	0.659	0.322	0.240	0.183
i-C$_4$H$_8$ inlet (ml min^{-1})	0.000	0.238	0.260	0.200	0.500	0.512
i-C$_4$H$_8$ outlet (ml min^{-1})	0.266	0.326	0.341	0.078	0.260	0.329
H$_2$ inlet (ml min^{-1})	0.000	0.000	0.000	0.600	0.500	0.488
H$_2$ outlet (ml min^{-1})	0.266	0.088	0.081	0.478	0.260	0.305
He flow (ml min^{-1})	68.24	67.12	91.85	68.24	67.12	90.27

Note. For each run, the marking level was 99.8%; gas volumes are given for NTP, i.e., 293 K and 1 atm.

$$\frac{\beta C_A}{W}\frac{dz_A}{dt} = -\left(\frac{F^A}{W} + v_{+1}\right)z_A$$
$$+ v_{-1}z_2 + \frac{F_f^A}{W} z_{in}^A, \quad (14)$$

$$C_4H_9l \,\frac{dz_2}{dt} = v_{+1}z_A$$
$$- (v_{-1} + v_{+2})z_2 + v_{-2}z_3, \quad (15)$$

$$C_4H_8l \,\frac{dz_3}{dt} = v_{+2}z_2$$
$$- (v_{-2} + v_{+3})z_3 + v_{-3}z_E, \quad (16)$$

$$\frac{\beta C_E}{W}\frac{dz_E}{dt} = v_{+3}z_3$$
$$- \left(\frac{F^E}{W} + v_{-3}\right)z_E + \frac{F_f^E}{W} z_{in}^E, \quad (17)$$

where the meaning of symbols is as defined in the Appendix.

Only five parameters must be evaluated. Two of them are the surface concentrations of i-C$_4$H$_9l$ and i-C$_4$H$_8l$ on the catalyst. The remaining three can be taken as v_{+1}, v_{+2}, and v_{+3}. The corresponding step velocities v_{-i} can be computed from the three v_{+i} because the overall rate of dehydrogenation V

$= v_{+i} - v_{-i}$ is independently determined. All parameters have been shown in (*11*) to be structurally globally identifiable.

Table 2 presents their values, estimated by unweighted nonlinear least-squares regression for several typical data sets. For each data set, the overall velocity was recorded as well as the fractional markings of both isobutane and isobutene as functions of time.

From results of this type, it was clear that the last step is very close to equilibrium, so we next considered a reduced model lumping the last two compartments to obtain the three-compartment model shown in Fig. 2b. The equations of the resulting *three-pool model* are

$$\frac{\beta C_A}{W}\frac{dz_A}{dt} = -\left(\frac{F^A}{W} + v_{+1}\right)z_A$$
$$+ v_{-1}z_2 + \frac{F_f^A}{W} z_{in}^A, \quad (18)$$

$$C_4H_9l\frac{dz_2}{dt} = v_{+1}z_A$$
$$- (v_{-1} + v_{+2})z_2 + v_{-2}z_E, \quad (19)$$

$$\left(\frac{\beta C_E}{W} + C_4H_8l\right)\frac{dz_E}{dt} = v_{+2}z_2$$
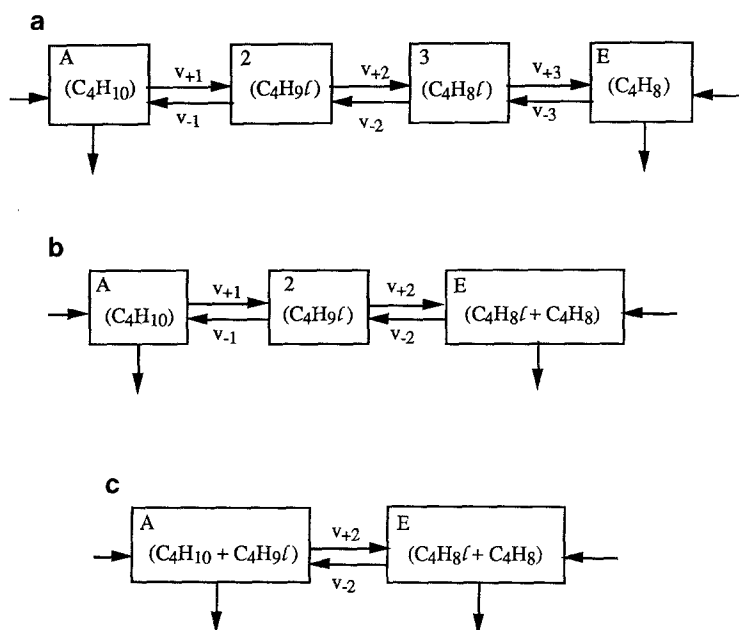$$- \left(\frac{F^E}{W} + v_{-2}\right)z_E + \frac{F_f^E}{W}z_{in}^A. \quad (20)$$

FIG. 2. Structures of proposed models.

In this case, the number of parameters is decreased by one. They are $i\text{-}C_4H_9l$, $i\text{-}C_4H_8l$, v_{+1}, and v_{+2}, and all of them are structurally globally identifiable (*11*). In Fig. 2b, C_4H_8 represents isobutene in the gas phase that corresponds to $\beta C_E/W$ in Eq. (20). We modeled a number of experiments including those listed in Table 1. Results are summarized in Table 3.

The parameters appearing in this reduced three-pool model are consistent with those of the original four-compartment model. The estimated velocity of $i\text{-}C_4H_{10}$ chemi-

sorption v_{+1} is still so high that it can be reasonably considered to be at equilibrium. Consequently we further reduced the model by lumping the first and second steps as shown in Fig. 2c.

The resulting *two-pool model* contains one less parameter and is described by

$$\left(\frac{\beta C_A}{W} + C_4H_9l\right)\frac{dz_A}{dt} = -\left(\frac{F^A}{W} + v_{+2}\right)z_A$$

$$+ v_{-2}z_E + \frac{F_f^A}{W}z_{in}^A, \quad (21)$$

TABLE 2

Parameters for the Four-Pool Model Estimated by Unweighted Least-squares

Run No.	C_4H_9l (ml g^{-1})	C_4H_8l (ml g^{-1})	v_{+1} (ml g^{-1} min^{-1})	v_{+2} (ml g^{-1} min^{-1})	v_{+3} (ml g^{-1} min^{-1})
0725A88	0.0396	0.0021	8750.9	0.0263	70981
1030B87	0.0258	0.0102	9572.2	0.0073	93062
0725B88	0.0093	0.0351	2623.8	0.0027	75210
1031B87	0.0074	0.0422	1025.8	0.0022	59666

Note. The first two runs are butane step-ups on dehydrogenation and the last two runs are butene step-ups on hydrogenation. All units are NTP.

KAO ET AL.

TABLE 3

Parameters for the Three-Pool Model Estimated by Unweighted
Least-Squares

Run No.	C_4H_9l (ml g^{-1})	C_4H_8l (ml g^{-1})	v_{+1} (ml g^{-1} min^{-1})	v_{+2} (ml g^{-1} min^{-1})
0725A88	0.0412	0.0013	9622.9	0.0241
0717A88	0.0232	0.0049	7333.8	0.0086
1030A87	0.0282	0.0033	877.98	0.0058
0725B88	0.0078	0.0236	2168.8	0.0011
0717B88	0.0068	0.0318	2387.6	0.0024
1031A87	0.0097	0.0296	1660.9	0.0013

Note. All units are NTP.

$$\left(\frac{\beta C_E}{W} + C_4H_8l\right)\frac{dz_E}{dt} = v_{+2}z_A$$

$$- \left(\frac{F^E}{W} + v_{-2}\right)z_E + \frac{F_f^E}{W}z_{in}^E. \quad (22)$$

The parameters to be estimated are now i-C_4H_9l, i-C_4H_8l, and v_{+2}; all of them are structurally globally identifiable (*11*). In Fig. 2c, $C_4H_{10} = \beta C_A/W$ and $C_4H_8 = \beta C_E/W$. Table 4 gives a typical comparison between the parameters estimated for the three-pool and two-pool models.

Table 5 gives the values for the parameters of the two-pool model estimated by unweighted least-squares from various runs involving hydrogenation and dehydro-

TABLE 4

Comparison between the Three- and Two-Pool Models for a Typical Run (Run 0717A88: Dehydrogenation of Isobutane at 629 K, Butane Step-Up)

Models	Three pools	Two pools
Parameters		
C_4H_9l (ml g^{-1})	0.0232	0.0237
C_4H_8l (ml g^{-1})	0.0049	0.0040
v_{+1} (ml g^{-1} min^{-1})	7333.8	—
v_{+2} (ml g^{-1} min^{-1})	0.0086	0.0086
V_+/V_-	2.573	2.599

Note. All units are NTP.

genation. Indicated in parentheses is a (rough) estimate of the standard deviations of the parameters obtained from the diagonal of the inverse of the Fisher information matrix. Again the parameters appearing in this two-pool model compare very closely with those obtained from the three- and four-pool models. This simplest model therefore gives results consistent with those of the more complex models. Moreover, it correlates the data in a manner almost identical to those with more complex structures. Figures 3 to 8 show measured versus calculated values for the observed tracer markings for the models presented in Table 5. Since these experiments used reactant marking, an immediate increase in reactant tracer fraction is observed. Product tracer fraction, on the other hand, exhibits a zero initial slope resulting in an S-shaped curve.

Given a suitable correlation of the data, the next question that arises concerns the reliability of the estimated parameters themselves. As discussed under Methods, separate additional treatment of the data was employed using the determinant criterion. This affords a less restrictive approach to parameter estimation. Table 6 gives the estimates $\hat{\theta}_{det}$ obtained for the parameters of the two-pool model by minimizing the determinant criterion for the same runs as those in Table 5. The corresponding estimated standard deviations are indicated in parenthe-

TABLE 5

Parameters for the Two-Pool Model Estimated by Unweighted Least-Squares

Run No.	C_4H_9l (ml g^{-1})	C_4H_8l (ml g^{-1})	v_{+2} (ml g^{-1} min^{-1})
0725A88	0.0411 (0.0017)	0.00155 (0.0018)	0.0243 (0.0013)
0717A88	0.0237 (0.00096)	0.00396 (0.0020)	0.00860 (0.00011)
1030A87	0.0289 (0.00071)	0.00468 (0.0016)	0.00559 (0.000051)
0725B88	0.00725 (0.0011)	0.0237 (0.00026)	0.00109 (0.000046)
0717B88	0.00646 (0.00082)	0.0321 (0.00071)	0.00222 (0.00036)
1031A87	0.0105 (0.00076)	0.0291 (0.00068)	0.00161 (0.00029)

Note. Numbers in parentheses are the corresponding standard deviations, estimated from the diagonal of the inverse of the Fisher information matrix.

ses. To compute $\hat{\theta}_{det}$, we used a global optimizer (12) implementing the adaptive random search strategy (13). This optimizer is capable of escaping local minima of the criterion and is thus much less sensitive than conventional local optimizers to the initial value for the parameters to be estimated. The prior feasible range for each parameter was chosen as [0, 1] and the initial value for θ was taken as the center of the corresponding feasible box, i.e., $\theta = (0.5, 0.5, 0.5)^T$. Using other initial values for the parameters, the same estimates were obtained. To keep the amount of computation within feasible limits, the estimates θ^k needed for the Monte

Carlo analysis were computed using a local optimizer with the initial value $\hat{\theta}_{det}$.

Although obtained under less restrictive hypotheses, results shown in Table 6 agree quite well with those determined using the unweighted least-squares criterion given in Table 5. The estimated standard deviations reported in Tables 5 and 6 are very small and indicate that the parameters are very precisely determined. However, their absolute accuracy relies on that of the statistical hypotheses made on the measurement error. Greater uncertainty, of course, exists for the values of the parameters themselves due to systematic errors in rate measure-
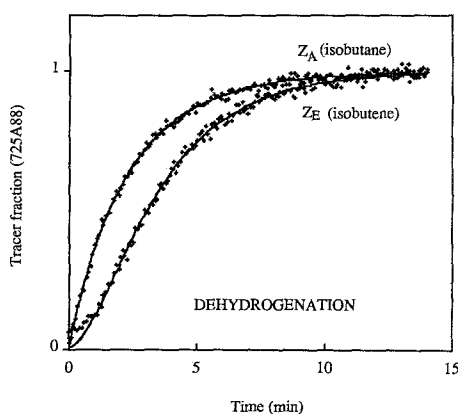

FIG. 3. Data and best two-pool model in the sense of unweighted least-squares for Run 0725A88.
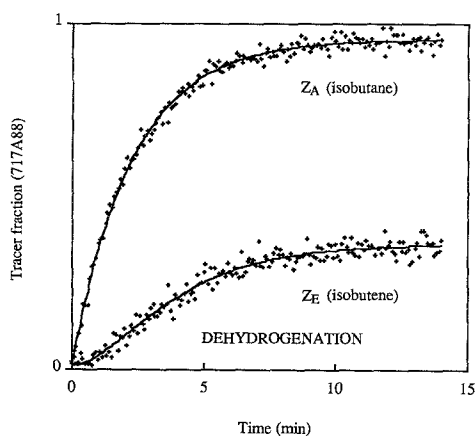
FIG. 4. Data and best two-pool model in the sense of unweighted least-squares for Run 0717A88.
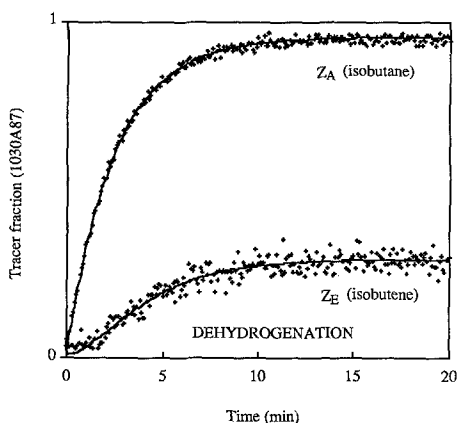
FIG. 5. Data and best two-pool model in the sense of unweighted least-squares for Run 1030A87.

FIG. 7. Data and best two-pool model in the sense of unweighted least-squares for Run 0717B88.

ments and component analyses that are always present when obtaining kientic data. We do not believe that measurement accuracy is better than ±5% with consequent errors in parameter estimation. Diffusional resistances for steps close to equilibrium introduce further uncertainties.

Because of the fact that the simulations of the outputs of the models described in Tables 5 and 6 are almost identical, the information presented in Figs. 3 to 8 also applies to the models described in Table 6.

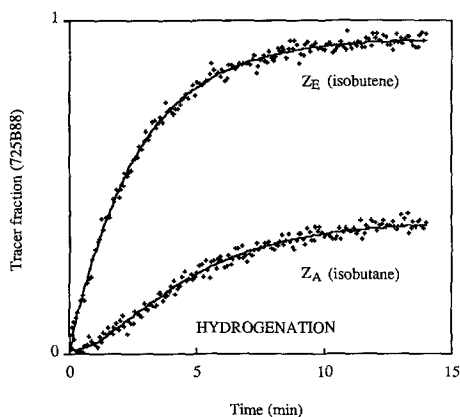As shown in Tables 2 to 6, employing several models and estimation methods, the

concentration of i-C_4H_9l species is higher than that of i-C_4H_8l during the dehydrogenation and the reverse is true during hydrogenation. Such an accumulation in a catenary reaction path is consistent with the simultaneous occurrence of small differences between values of rate constants for forward and reverse velocities of the rate-controlling step, along with small differences between the concentrations of unoccupied catalyst sites and those occupied by chemisorbed hydrogen atoms.

Additional auxiliary experiments were conducted to furnish independent confir-

FIG. 6. Data and best two-pool model in the sense of unweighted least-squares for Run 0725B88.
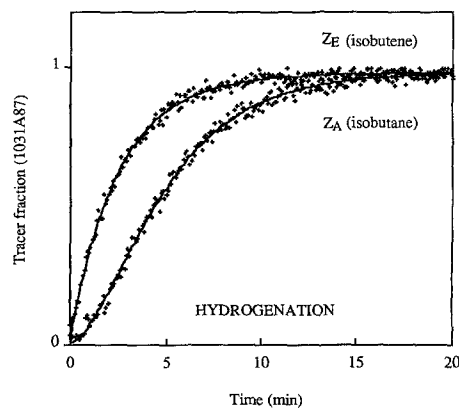

FIG. 8. Data and best two-pool model in the sense of unweighted least-squares for Run 1031A87.

TABLE 6

Parameters for the Two-Pool Model Estimated by the Determinant Criterion

Run No.	C_4H_9l (ml g^{-1})	C_4H_8l (ml g^{-1})	v_{+2} (ml g^{-1} min^{-1})
0725A88	0.0406 (0.00060)	0.00210 (0.00051)	0.0248 (0.00051)
0717A88	0.0237 (0.00139)	0.00410 (0.00209)	0.00861 (0.00014)
1030A87	0.0283 (0.00072)	0.00761 (0.00061)	0.00574 (0.00008)
0725B88	0.00740 (0.00074)	0.0236 (0.00041)	0.00110 (0.00007)
0717B88	0.00648 (0.00060)	0.0320 (0.00061)	0.00222 (0.00037)
1031A87	0.0106 (0.00109)	0.0289 (0.00098)	0.00166 (0.00041)

Note. Numbers in parentheses are the corresponding standard deviations, estimated by the Monte Carlo method.

mation of the high rates of interaction of terminal species with the catalyst. The reactor system was reduced with hydrogen for several hours and purged with helium at a temperature of 523 K, considerably below temperatures employed for hydrogenation–dehydrogenation experiments. Following this a step function is introduced consisting of a mixture of deuterium and isobutane. In less than 10 s, HD as well as multiple i-$C_4H_xD_{10-x}$ species were observed in the effluent, showing that hydrogen and hydrocarbon exchanges are very rapid.

Experiments were also conducted to furnish independent information concerning adsorbed species. The catalyst was reduced and purged with helium as described under experimental procedure. A mixture of argon and isobutene in the ratio 1 : 1 together with helium carrier gas was then passed over the catalyst as 338°C (15–20°C lower than the usual hydrogenation–dehydrogenation experiments). A delay in isobutene concentration appearance in the CSTR was observed. This was considered to be due to adsorption of isobutene from the gas phase. The difference between the curves for isobutene and argon was integrated and corresponded to 0.08 ml NTP g^{-1}. At the end of this adsorption period the flow of the argon–isobutene mixture was stopped and the system was purged with He carrier gas until no isobutene would be detected in the effluent. The purpose of this procedure was to remove

physically adsorbed isobutene, leaving isobutene chemisorbed on active catalyst sites. Hydrogen was then injected into the CSTR at a rate of 4 ml NTP min^{-1} along with carrier gas. Two or three min after hydrogen injection commenced, isobutane was observed in the effluent and this phenomenon proceeded for about 6 min as shown in Fig. 9. By integrating the isobutane curve with respect to time, the amount of chemisorbed isobutene reacted with hydrogen was found to correspond to 0.04 ml NTP g^{-1}. This corresponds approximately with values reported in Tables 5 and 6 for the sum of concentrations of i-C_4H_8l and i-C_4H_9l. In regular tracer experiments less than 1% of CH_4 relative to C_4's was detected in the effluent, indicating absence of cracking. No methane or other hydrocarbons were detected in the adsorption experiments. Isobutane in contrast to isobutene adsorbs dissociatively producing hydrogen, adsorption of which can then compete for surface sites, so interpretation of results is more complicated in that case and there is less hydrocarbon adsorption (about 0.02 ml NTP g^{-1} at 337°C).

DISCUSSION

The catalytic properties of chromia have been studied extensively by Burwell and co-workers (14–16) and Molina (17), so it is of interest to compare their findings with those of this study.

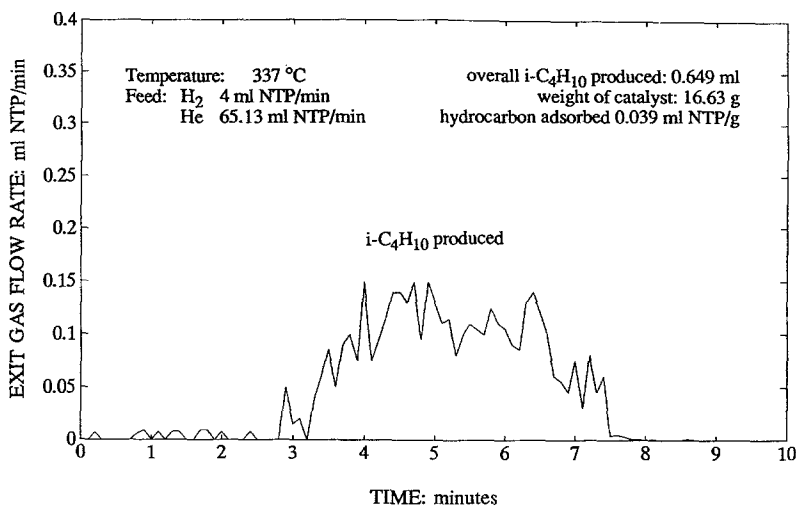On the basis of results for deuterium ex-

FIG. 9. Hydrogen washing experiment.

change, Burwell et al. (14, 15) concluded that the primary hydrogen atoms in propane are at least six times more reactive than the secondary ones over chromia gel catalyst. It appears that the nine primary hydrogen atoms on the rotating H_3C-C groups in isobutane are more likely than the single tertiary hydrogen atom of an isobutane molecule to contact the catalyst surface, so that sterochemical effects should be even more pronounced than in the case of propane. In the case of isobutane additional energy would also be required to change the tetrahedral ($i-C_4H_9l$) structure to the planar ($i-C_4H_9l$) form, which is an important factor in explaining the relatively slow rate of this step observed in our studies.

As regards surface concentrations of adsorbed species, the amorphous chromia prepared by us has approximately the same surface area by the BET method as that used by Burwell et al. (16) and Molina (17). These authors considered that the irreversible adsorption of carbon monoxide constituted a suitable measure of active sites and reported values of 1.1 molecules/100 $Å^2$ for amorphous chromia. This corresponds to adsorption of 11.4 ml NTP g^{-1} of catalyst which is decidedly larger than the 0.04 ml NTP g^{-1} occupied by the sum of $i-C_4H_8l$ and $i-C_4H_9l$

intermediates in our studies. The partial pressures of reacting species are much lower than atmospheric pressure in our case. This fact along with the shapes of isobutane and isobutene molecules may contribute to this difference in behavior.

It is of interest to compare the values of V_+/V_- reported in Table 4 with those predicted from relationships based on transition state theory and thermodynamics (Happel (1))

$$\frac{V_+}{V_-} = \frac{\prod_i v_{+i}}{\prod_i v_{-i}} = \exp(-\Delta G/RT)$$

$$= \frac{K_p \cdot p_{i-C_4H_{10}}}{p_{H_2} \cdot p_{i-C_4H_8}}. \quad (23)$$

Using data from experiments on the isobutane–isobutene–hydrogen system over chromia alumina catalyst, similar to those reported earlier (Happel et al., (18)) we estimated that for the conditions given in Table 4 V_+/V_- should equal 2.433 based on the observed temperature of 629 K. The values in Table 4 are about 5% higher, corresponding to a predicted temperature of about 630 K. This is better agreement than would be expected considering experimental accuracy. It does provide further corroboration

of the theory as well as providing evidence that the system was operating at isothermal conditions.

Perhaps the most important result from this study is the demonstration that a reversible reaction can be well modeled using transient tracing regardless of how overall kinetics may be correlated (*19*). These results were obtained by using several quite different types of experiments as well as an improved statistical treatment of the data. Evidence is presented for the existence of a dual-site mechanism for isobutane dehydrogenation with a single rate-controlling step involving interconversion of i-C_4H_9l and i-C_4H_8l.

Very often reaction kinetics have been modeled on the basis of the so-called Langmuir–Hinshelwood–Hougen–Watson (LHHW) method, which assumes both a single rate-controlling step and catalyst surface uniformity. Experimental results are modeled on the basis that the identity of the rate-determining step itself is an unknown parameter to be identified. The large number of parameters often involved in such modeling makes identification of the rate-determining step and concentrations of intermediates uncertain. The procedure used in this study avoids these problems.

APPENDIX: NOMENCLATURE

C_A Volumetric fraction of butane in the gas phase (measured constant).

C_E Volumetric fraction of butene in the gas phase (measured constant).

C_4H_8l Concentration of i-C_4H_8l on the catalyst surface per unit mass of catalyst, in ml (NTP) g^{-1} (parameter to be estimated).

C_4H_9l Concentration of i-C_4H_9l on the catalyst surface per unit mass of catalyst, in ml (NTP) g^{-1} (parameter to be estimated); NTP is 293 K and 1 atm.

$D(\theta)$ Two-by-two matrix, the determinant of which is to be minimized.

det D Determinant of the matrix D.

F^A Rate of removal of butane from the system, in ml (NTP) min^{-1} (measured constant).

F_f^A Rate of feed of butane to the system, in ml (NTP) min^{-1} (measured constant).

F^E Rate of removal of butene from the system, in ml (NTP) min^{-1} (measured constant).

F_f^E Rate of feed of butene to the system, in ml (NTP) min^{-1} (measured constant).

ΔG Gibbs free-energy change for overall reaction.

i-C_4H_8 Isobutene.

i-C_4H_8l Chemisorbed isobutene.

i-C_4H_9l Half-hydrogenated chemisorbed species

i-C_4H_{10} Isobutane.

$j(\theta)$ Criterion to be minimized with respect to the parameter vector θ.

K_p Equilibrium constant, in pressure units.

l Site for chemisorption.

N Number of measurement times.

$n_s(t_i)$ Simulated measurement errors.

$n(t_i)$ Measurement errors.

p_x Partial pressure of x, in atm.

R Gas constant.

T Absolute temperature, in K.

t Time, in min.

t_i Measurement time, in min.

v_{+i} Reaction velocities of the ith individual step (i = 1, 2, 3), in ml (NTP) g^{-1} min^{-1} (parameters to be estimated).

V Overall rate of dehydrogenation per unit mass of catalyst, in ml (NTP) g^{-1} min^{-1} (measured constant).

V_+ Overall forward velocity (dehydrogenation), $\prod_i v_{+i}$.

V_- Overall backward velocity (hydrogenation), $\prod_i v_{-i}$.

W Total mass of catalyst in the system, in g (measured constant).

$y(t_i)$ Two-dimensional vector of tracer fractions for isobutane and isobutene observed at time t_i.

$\mathbf{y}_m(t, \boldsymbol{\theta})$ Two-dimensional vector of the model outputs corresponding to $\mathbf{y}(t)$.

$\mathbf{y}_s(t)$ Two-dimensional vector of simulated data.

z_A, z_E Atomic fraction of tracer in butane and butene (measured state variables).

z_{in}^A, z_{in}^E Input fractional tracer level in butane and butene (measured). In our experiments, either z_{in}^A or z_{in}^E was chosen as a step function.

z_i Atomic fraction of tracer in compartment i ($i = 2, 3$) (not measurable state variables).

β Dead space of the system, in ml (NTP) (measured).

$\boldsymbol{\theta}$ Unknown parameters of the model to be estimated from the data.

$\langle \theta_i \rangle$ Estimated mean of the ith component of $\boldsymbol{\theta}$.

$\boldsymbol{\theta}^k$ Pseudo estimate of $\boldsymbol{\theta}$ obtained from simulated data.

$\hat{\boldsymbol{\theta}}_{det}$ Estimate of the parameters obtained with the determinant criterion.

σ_i Estimated standard deviation of the ith component of $\boldsymbol{\theta}$.

$\boldsymbol{\Sigma}$ Covariance matrix of the measurement noise.

$\hat{\boldsymbol{\Sigma}}_{ml}$ Maximum likelihood estimate of $\boldsymbol{\Sigma}$.

ACKNOWLEDGMENTS

REFERENCES

1. Happel, J., "Isotopic Assessment of Heterogeneous Catalysis." Academic Press, Orlando, FL, 1986.
2. Happel, J., Kao, J.-Y., Yoshikiyo, M., Chen, Z., Takeyasu, O., Hnatow, M. A., Cheh, H. Y., Walter, E., and Lecourtier, Y., in "Proceedings, 9th International Congress on Catalysis, Calgary, 1988" (M. J. Phillips and M. Ternan, Eds.), p. 1457. Chem. Institute of Canada, Ottawa, 1988.
3. Emmett, P. H., and Cines, M., J. Am Chem. Soc. 68, 2535 (1946).
4. Kao, J-K., Ph.D thesis, Columbia University, pp. 35, 44, 1989.
5. Happel, J., Cheh, H. Y., Otarod, M., Ozawa, S., Severdia, A. J., Yoshida, T., and Fthenakis, V., J. Catal. 75, 314 (1982).
6. Box, G. E. P., and Draper, N. R., Biometrika 52, 355 (1965).
7. Goodwin, G. C., and Payne, R. L., "Dynamic System Identification: Experiment Design and Data Analysis," pp. 88–93. Academic Press, New York, 1977.
8. Froment, G. F., Chem. Eng. Sci. 42, 1073 (1987).
9. Press, W. H., Flannery, B. P., Teukolsky, S. A., and Vetterling, W. T., "Numerical Recipes, the Art of Scientific Computing." Cambridge Univ. Press, Cambridge, 1986.
10. Horiuti, J., and Polanyi, M., Trans. Faraday Soc. 30, 663, 1164 (1934).
11. Walter, E., Lecourtier, Y., Kao, J.-Y., and Happel, J., Chem. Eng. Comm. 83, 157 (1989).
12. Pronzato, L., Walter, E., Venot, A., and Lebruchec J.-F., Math. Comput. Simul. 26, 412 (1984).
13. Bekey, G. A., and Masri, S. F., Math. Comput. Simul. 25, 210 (1983).
14. Burwell, R. L., Jr., Littlewood, A. B., Cardew, M., Pass, G., and Stoddart, C. T. H., J. Am. Chem. Soc. 82, 6272 (1960).
15. Pass, G., Littlewood, A. B., and Burwell, R. L., Jr., J. Am. Chem. Soc. 82, 6281 (1960).
16. Burwell, R. L., Jr., Haller, G. L., Taylor, K. C., and Read, J. F., in "Advances in Catalysis" (D. D. Eley, H. Pines, and P. B. Weisz, Eds.), Vol. 20, p. 6281. Academic Press, New York, 1969.
17. Molina, A., Ph.D. thesis, Yale University, 1984.
18. Happel, J., Kamholz, K., Walsh, D., and Strangio, V., I & EC Fundam. 12, 263 (1983).
19. Happel, J., Walter, E., and Lecourtier, Y., I & EC Fundam. 25, 704 (1986).